Sediment Transport and Associated Long-term Bathymetric Changes due to Tidal Currents in The Seto Inland Sea, Japan

Ubara, Motoki

Uchiyama, Yusuke

Kosako, Taichi

(Citation)
IOP Conference Series: Earth and Environmental Science,945(1):012041

(Issue Date)
2021-12-21

(Resource Type)
journal article

(Version)
Version of Record

PAPER • OPEN ACCESS

Sediment Transport and Associated Long-term Bathymetric Changes due to Tidal Currents in The Seto Inland Sea, Japan

To cite this article: Motoki Ubara *et al* 2021 *IOP Conf. Ser.: Earth Environ. Sci.* **945** 012041

Sediment Transport and Associated Long-term Bathymetric Changes due to Tidal Currents in The Seto Inland Sea, Japan

Motoki Ubara, Yusuke Uchiyama* and Taichi Kosako

Department of Civil Engineering, Kobe University, Kobe, Japan

*Corresponding author's e-mail: uchiyama@harbor.kobe-u.ac.jp

Abstract. The topography of the seafloor is essential for determining physical phenomena such as ocean currents, favorable habitats for marine organisms, optimal vessel navigation, and so on. Prevailing currents and waves, as well as associated shear stresses acting on the ocean floor, are responsible for the formation of typical topographic features including sea caldrons and sandbanks through erosion of bedrock and sediments and their deposition processes. In the Seto Inland Sea (SIS), the most extensive semi-enclosed estuary in Japan, tidal currents affect pronouncedly the formation of seafloor topographic features; however, they have not been fully studied, particularly from a hydrodynamic viewpoint. This study aims to understand bathymetric formation under the predominance of tidal currents in the SIS. A 3-D high-resolution SIS circulation model based on the JCOPE2-ROMS system in a triple-nested configuration was utilized to examine the detailed hydrodynamic processes for the topography formations. A high correlation between the bottom shear stress and the scour depth of the erosive areas was observed, demonstrating that local tidal forcing has continuously been exerted on the seafloor to erode. A diagnostic sediment budget analysis was then conducted for sediments typical of the SIS, that is, gravel, sand, and clay, using the modeled circulation field. The horizontal divergence of the residual flows indicates consistency between divergence (convergence) and erosion (deposition). The sediment budget model also shows that these sediments are generally transported from deep to shallow areas in eroded terrains to form deposited terrains fringing the eroded terrains, whereas sedimentation tendency differs largely from location to location.

Keywords: caldron; sandbank; tidal estuary; sediment transport; ROMS.

1. Introduction

The topography of the seafloor, which accounts for 70% of the earth's total surface area, plays an important role in many marine phenomena such as hydrodynamics and resultant ecosystems [1-3]. In the Seto Inland Sea (SIS; **Figure 1**), the most extensive semi-enclosed estuary in Japan, there are mainly two types of seafloor topography formed by tidal currents: caldron, formed by erosion of the seafloor, and sandbank, formed by sediment deposition in areas where the currents around the straits are slow [4]. In particular, sandbanks are home to organisms that prefer sandy seabeds such as sand lance and juvenile anchovy [5], and are good fishing grounds for a variety of fish. However, many sandbanks and sandy seabeds have been lost because of the extraction of large amounts of marine sand as concrete aggregate for building and infrastructure construction during the Japan's economic growth period of the 1960s [6]. It is necessary to clarify the source of sediment supply, formation process, and origin of sandbanks in order to investigate the possibility of restoring lost sediments and eroded topographies. These unique topographies evolve on multiple timescales ranging from a single storm or a tidal cycle (hours to days)

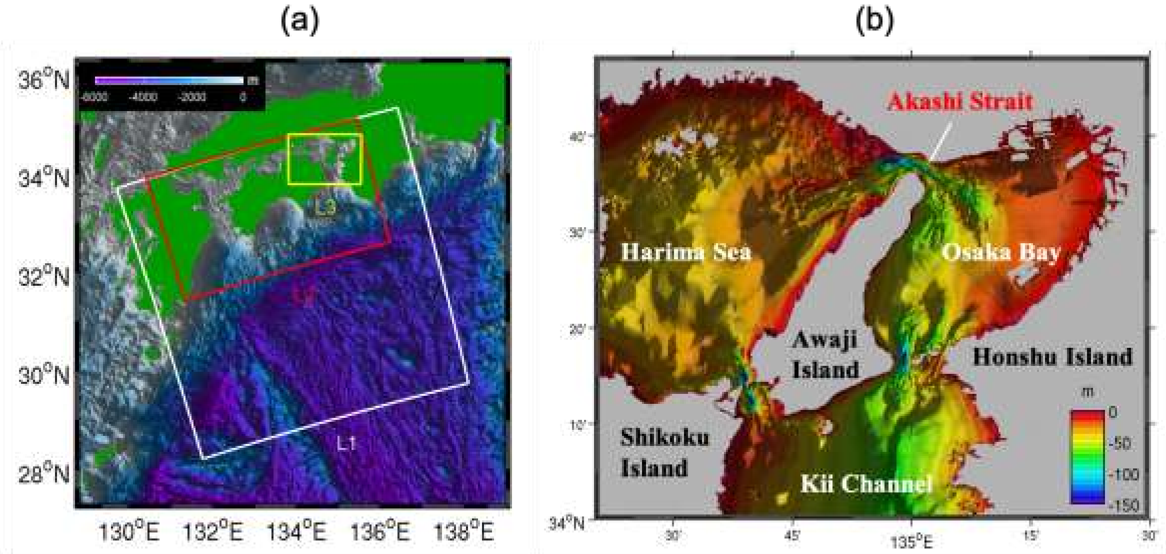

Figure 1. (a) Hierarchy of the quadruple nested JCOPE2-ROMS downscaling model domain around the Seto Inland Sea and bathymetry (color: m). The colored rectangle frames account for ROMS-L1 (white, at lateral grid resolution of 2 km), L2 (red, 600 m), and L3 (yellow, 200 m). (b) Enlarged domain of the relief of the seafloor topography in the eastern Seto Inland Sea comprising Harima Sea, Osaka Bay, and Kii Channel in the ROMS-L3 model.

to geological spans (thousands of years or longer) under the potential influences of human activities such as construction of dams that diminish terrestrial sediment supply to the sea. Their shape classification and long-term formation mechanism have been the focus of marine geologists [7]. However, because of their temporal and physical complexity in external forcing, including ambient currents, most geological studies lack quantitative considerations from a hydrodynamic perspective to understand bathymetric changes. In contrast, in the field of coastal engineering, marine sediment transport and associated morphological processes are generally investigated in much shorter timescales from days to decades, with quantitative considerations of hydrodynamic effects from waves and currents as accurately as possible. Therefore, bridging the gap between geological and engineering timescales is quite challenging, whereas such attempts have never been made to understand long-term topographic changes in caldrons and sandbanks in the SIS by considering detailed background currents and resultant sediment transport processes.

In this study, the formation mechanisms of topographies typical of tidal straits such as sandbanks and caldrons in the eastern SIS, Japan, was investigated. In particular, conventional marine geological approaches are combined with quantitative, detailed, and dynamically consistent methods that have been developed in the field of coastal engineering to examine the relationship between seafloor morphological processes and ambient tidal currents responsible for regional sediment transport. To this end, a state-of-the-art high-resolution ocean circulation model specifically designed for the eastern SIS was exploited using a multi-nesting technique that enables us to quantify the tidally averaged forcing exerted on the seafloor. Based on the circulation model outputs, such as 3D velocity fields and associated bed shear stress, a diagnostic depth-integrated sediment transport model was developed to analyze sediment resuspension from the seafloor, short-term lateral sediment transport due to suspended load and bed load, and consequent deposition and erosion of the bed topography.

2. Nested Ocean Circulation Model and the Diagnostic Morphology Model

A quadruple-nested downscaling model based on the Regional Oceanic Modeling System (ROMS [8]) was employed along with assimilative Japan Coastal Ocean Predictability Experiments (JCOPE2) oceanic reanalysis [9]. The lateral boundary and initial conditions for the outermost ROMS-L1 model

Table 1. Numerical configuration of ROMS-L3

Computational period	December 25, 2011-March 3, 2012
Grid cell numbers	800× 560 × 32 vertical s-layers, lateral grid resolution: 200 m
Lateral boundary conditions	ROMS-L2 (2-hourly average)
Surface wind stress	Japan Meteorology Agency GPV-MSM (hourly)
Other surface fluxes	COAMPS bulk formula
Sea surface temperature (SST)	JCOPE2 (20-day averaged)
River discharge	10 major rivers
Bathymetry	Central Disaster Prevention Council, Japan (50 m resolution).

Table 2. Model parameters for the multi-class sediment transport model

class	d mm	ρ_s $\mathrm{kgm^{-3}}$	w_s $\mathrm{mms^{-1}}$	E_u $\mathrm{kgm^{-2}s^{-1}}$	τ_{cr} $\mathrm{Nm^{-2}}$
gravel	2	2650	170	1×10^{-4}	1.26
sand	0.125	2650	9.4	1×10^{-4}	0.15
silt	0.024	2650	0.4	1×10^{-4}	0.07
clay	0.004	2650	0.1	1×10^{-4}	0.02

where d: median grain size, ρ_s: sediment dry density, w_S: settling velocity, E_u: resuspension rate, τ_{cr}: critical bed shear stress for resuspension.

were provided by JCOPE2 (**Figure 1**). The one-way offline nesting technique [10] was used to downscale the parent model results in the corresponding child models with successive grid-size refinement (i.e., JCOPE2 at lateral grid resolution of 10 km → L1 at 2 km → L2 at 600 m → L3 at 200 m for the eastern SIS region). The numerical configurations for the inner-most ROMS-L3 model used in this study are listed in **Table 1**. The bottom shear stress governing resuspension of seafloor sediments was calculated from the frictional velocity using the conventional logarithmic law of wall turbulence. The divergence of the residual flow was also calculated to infer the averaged tendency of divergence and convergence of the fluid mass that is related to sediment accretion and erosion.

Furthermore, a diagnostic suspended sediment budget model for multi-sized non-cohesive sediment classes was developed using a precomputed ROMS-L3 3-D velocity field. A simple sediment transport and morphology model was constructed to evaluate the short-term sediment budget in a depth-integrated, horizontal two-dimensional sense. The depth-averaged sediment concentration $\overline{c_j}$ ($\mathrm{kgm^{-3}}$) may be expressed as

$$\overline{c_j} = \frac{1}{H}\int (E_j - D_j)dt, \tag{1}$$

where H is the total height (m) of the water column from the bed to the free sea surface. Our assumption is that the sediment concentration in a vertical water column is uniform and dynamically balanced instantaneously by the erosion flux E_j (kg m^{-2} s^{-1}) and the deposition flux D_j (kg m^{-2} s^{-1}) at the seafloor. Note that the subscript j denotes the sediment class of interest. The divergence of the depth-integrated suspended sediment fluxes induces a bed elevation change based on the following equation:

$$\Delta h_j = \frac{1}{\rho_s}\mathrm{div}\left(H\overline{c_j}\overline{\mathbf{u}}\right), \tag{2}$$

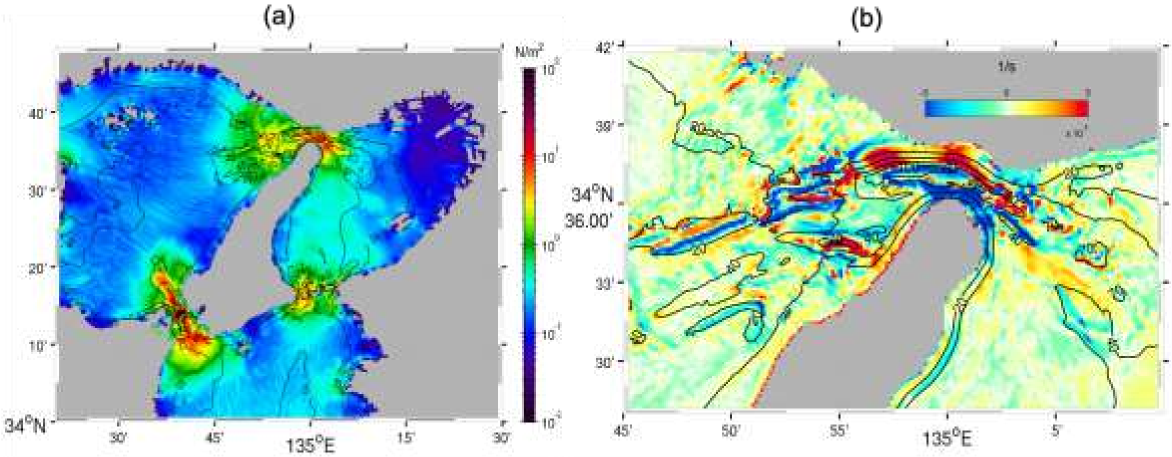

Figure 2. (a) Maximum value of the bottom shear stress during the calculation period (color: N/m^2). (b) Divergence of the bottom residual current for 70 days in color and black contours are isobaths in m around the Akashi Strait. Reddish colors indicate divergence, while bluish colors indicate convergence.

where Δh_j is the sedimentation (positive) or erosion (negative) rate (m s^{-1}) due to the j-th sediment class, $\bar{\mathbf{u}} = (\bar{u}, \bar{v})$ is the depth-averaged horizontal velocity (m s^{-1}), and ρ_s is the sediment dry density (kg m^{-3}). The erosion and deposition fluxes were evaluated based on the model proposed by Blaas et al. (2007) [11]. In this diagnostic model, bed sediments are re-suspended in water when the bed shear stress exceeds the critical shear stress for each sediment class. In the present analysis, four sediment classes (gravel, sand, silt, and clay) were considered with the model parameters listed in **Table 2**. The spatial distribution of sediment particle size composition was initially provided based on the observed data set collected *in situ* in the 2015-2017 investigation conducted by the Ministry of the Environment, Japan.

3. Hydrodynamics: Bed Shear Stress and Divergence of Bottom Currents

In **Figure 2a** the maximum value of the bottom shear stress τ_{bmax} for approximately five spring-neap cycles is shown. In general, τ_{bmax} is larger near the narrow straits and smaller in the bay and shallow areas. This result suggests that erosion occurs mainly around the straits. Further, the relationship between the maximum scour depth of the erosive topography and τ_{bmax} was examined. As a result, the correlation coefficient was evaluated to be 0.756 (not shown here), indicating a strong correlation between the bed stress and erosion depth. Marine geologists usually deduce that such caldrons may be caused by inundation of the previously depressed topography over a geological time scale. However, this result suggests that the caldrons were most likely formed by erosion of the seafloor due to near-bed currents.

In a semi-enclosed tidal estuary, current conditions change drastically in a short period of time, although residual currents exhibit time-averaged flow structures responsible for net sediment transport. Thus, the divergence of residual currents in the bottom layer, which are the time-averaged currents, was analyzed to exclude high-frequency tidal components. Since the overall trends of the hydrodynamics are similar in the three straits (i.e., the Akashi Strait to the north, the Naruto Strait between Shikoku and Awaji Islands to the west, and the Kitan Strait between the Awaji and Honshu Islands to the east) in the eastern SIS, we focus on the Akashi Strait as a representative in this paper (**Figure 2b**). Divergence (reddish) was observed in the northern part of the central caldron and the Todoroki-oki caldron to the west of the strait. On the other hand, convergence (bluish) is detected in the southern part of the central scour, where the depth steeply becomes shallower, and in the sandbanks on the east and west sides of

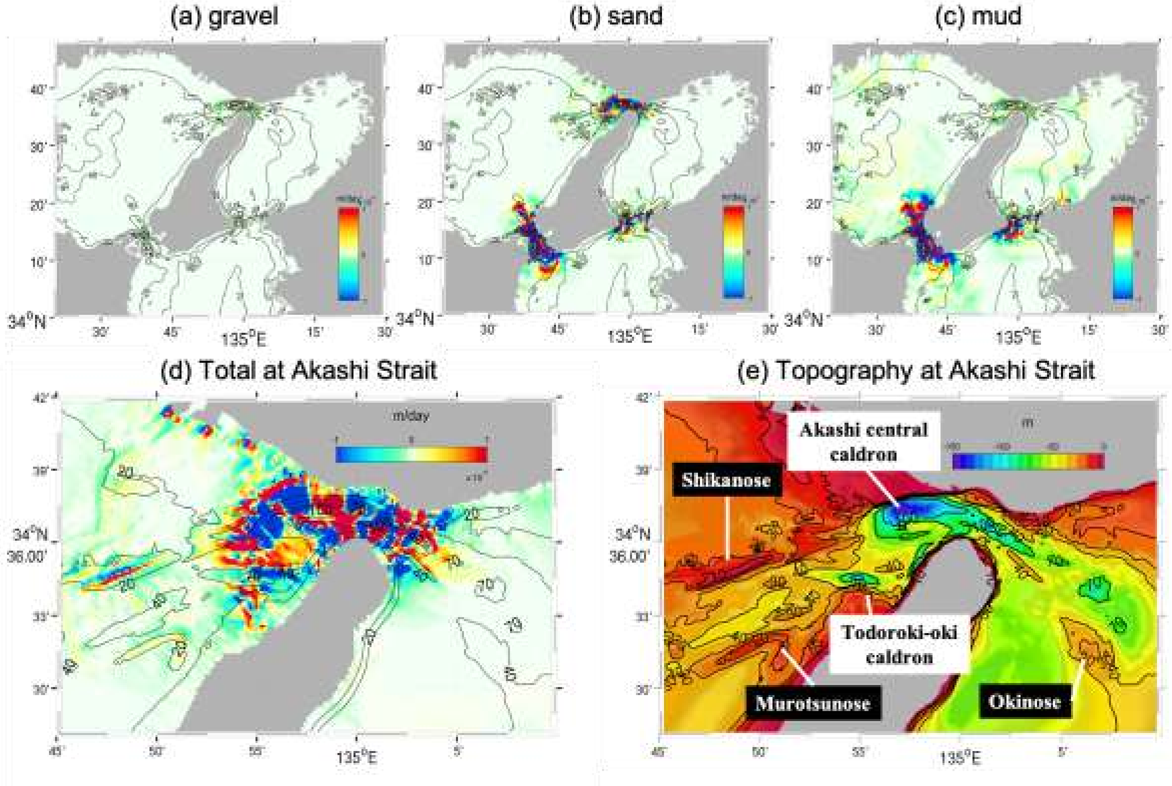

Figure 3. (a)-(d) Daily mean values of *Δh* (m/day, color) and isobaths (black contours) for 30 days from December 25, 2011 to January 23, 2012. Reddish colors indicate sedimentation, while bluish colors indicate erosion. The results are depicted for (a) gravel, (b) sand, (c) mud (i.e., silt + clay), and (d) total of all the four sediment classes around the Akashi Strait. (e) Topography of the seafloor around the Akashi Strait (bathymetry, color: m) and the names of each topography. The black letters indicate the names of erosive caldron topographies, whereas the white letters indicate the names of accretive sandbank topographies.

the strait. In other words, a divergent outflow occurs near the center of the scour hole, whereas convergent inflow occurs around the fringes of the scour and in the sandbanks.

4. Sediment Transport and Bathymetric Changes

In **Figure 3**, the spatial distribution of the daily averaged sediment accumulation rate *Δh* in m/day for each sediment class over 30 days in winter using the diagnostic sediment transport model is shown. Note that “mud” in **Fig. 3c** represents the sum of the silt and clay classes. In the erosive areas (bluish), where resuspension was dominant, gravel (**Figure 3a**) appeared only in the center of the strait, sand (**Figure 3b**) was scattered around the strait, and mud (silt + clay, **Figure 3c**) occurred not only in the strait but also in wide areas, including the inner and central areas of the bays where the bed shear stresses are small (**Figure 2a**). Although the smaller sediment grains are more broadly dispersed owing to the difference in settling velocity, the distribution of the erosion area was similar in all four sediments. **Figure 3d** shows the sedimentation rate for all four sediment classes by focusing on the Akashi Strait as a representative. Around the central caldron, bluish erosive areas prevail in the eastern part of the caldron at a depth of 110 m, the western part at a depth of 140 m, and the Todoroki-oki caldron to the southwest. However, reddish accumulative areas were formed in the central part of the caldron at a depth of 90 m, and in the north of the Todoroki-oki caldron. Because topographic sand waves were observed at the edge of the caldron [7], it is suggested that the eroded sediments in the caldron are transported to shallower areas fringing the caldron.

As seen in the sedimentation rate and the bed topographies away from the central strait, the two sandbanks in the western part of the strait (viz., Shikanose and Murotsunose) have gradually accumulated due to convergent sedimentation. On the other hand, the Okinose sandbank in the eastern part of the strait does not indicate any substantial remote effects associated with lateral sediment transport. However, a previous numerical study [12] suggested that the sediment particles artificially supplied in the west side of the strait are transported eastward at every eastward tidal current, gradually entrained in the clockwise residual circulation called “Okinose circulation” and eventually deposited on the Okinose sandbank. This long-term eastward sediment transport process might be a possible reason for the very slow sediment deposition observed at the Okinose sandbank.

The formation and origin of the sandbanks on the west and east sides of the Akashi Strait may be closely related to the formation process of the Akashi Strait occurring on a geological time scale. Based on a geological exploration, Yashima (1994) [7] estimated that the Akashi Strait was formed about 10,000 years ago, when the mean sea level was lowered to a depth of −30 m for the colder climate in that era. Yashima (1994) [7] further compared the paleotopography with the present one to conclude that the formation of the caldrons around the Akashi Strait began about 8,000 years ago, when the sea level was −20 m. Based on these geological considerations, close attention was paid to paleotopography when the sea level was −20 m. As a result, it was confirmed that these two western sandbanks were located at the westernmost part of the tidal channel and near the tip of the ancient cape-like topography that emerged 8,000 years ago. This suggests that the western sandbank may begin to form at about the same time as the Akashi Strait began to be eroded to supply sediments from the ancient narrow channel. In contrast, because there is no prominent source of sediments in the eastern part of the strait, the Okinose sandbank might have formed along with the formation of Osaka Bay, which allows the formation of residual flow due to the subsequent sea level rise in the last 8,000 years.

5. Conclusions

A quadruple nested, high-resolution tidal circulation model based on the JCOPE2-ROMS system was used to analyze the hydrodynamics and associated sediment transport and morphological processes in the eastern Seto Inland Sea, Japan. Our primary focus was on how the detailed hydrodynamics is responsible for the formation of caldrons and sandbanks near the tidal strait where the re-suspension potential is very large, which is usually omitted in traditional marine geological approaches. The estimated maximum bed shear stresses agree well with the amount of erosion that occurred in the caldrons. The near-bed residual flow and its divergence also capture the erosive and accretive nature of the seabed near the topographies around the straits. A simplified depth-integrated offline sediment budget model shows that sediment is greatly supplied from the deeper part of the caldron towards the fringing shallower areas to steepen the caldrons. However, the formation process of the sandbanks requires consideration of the long-term geological history of the strait.

Acknowledgements

The present research was financially supported by the Japan Society for the Promotion of Science (JSPS) Grants-in-Aid for Scientific Research 18H03798 (PI: Y. Uchiyama) at Kobe University. Special thanks are also due to the Ministry of the Environment, Japan, for supplying the in-situ data from their 2015-2017 investigation in the Seto Inland Sea.

References

[1] Uchiyama, Y., McWilliams, J.C., Akan, C.: Three-dimensional transient rip currents: Bathymetric excitation of low-frequency intrinsic variability. Journal of Geophysical Research: Oceans. 122 (2017) 5826-5849. https://doi.org/10.1002/2017JC013005

[2] Nishikawa, T., Okamoto, S.: Annual variation in condition factor of sand lance Ammodytes japonicus during the estivation period in Harima-Nada, eastern Seto Inland Sea,

Japan. Regional Studies in Marine Science. 42 (2021) 101644. https://doi.org/10.1016/j.rsma.2021.101644

[3] Izumi, T., Kitada, T., Kanaguchi, T., Fujihara, M.: Effects of infilling a sea caldron on tidal currents and seaweed and seagrass bed habitats. Journal of Rainwater Catchment Systems 22 (2017) 1-7. https://doi.org/10.7132/jrcsa.22_2_1

[4] Yanagi, T.: Currents and sediment transport in the Seto Inland Sea, Japan. In: Cheng R.T. (eds) Residual Currents and Long-term Transport. Coastal and Estuarine Studies. Springer, New York, NY, (1990) 348-355. https://doi.org/10.1007/978-1-4613-9061-9_24

[5] Genkai-Kato, M., Onishi, M., Doi, H., Nozaki, K., Yoshino, K., Miyasaka, H., Omori, K.: Photosynthetic property and primary production of phytoplankton in sublittoral sand bank area in the Seto Inland Sea, Japan. Ecological Research 23 (2008) 1025-1032. https://doi.org/10.1007/s11284-008-0472-6

[6] Tanabe, H., Takahashi, S., Murakami, K.: Relationship between sand bank topography and tidal residual flow in the Seto Inland Sea. Asian and Pacific Coasts 2003 (2004) 1-10.

[7] Yashima, K.: A geomorphological study of the caldrons in the Seto Inland Sea. Report of Hydrographic and Oceanographic Researches 30 (1994) 237-327 (in Japanese with English abstract).

[8] Shchepetkin, A.F., McWilliams, J.C.: The regional ocean modeling system (ROMS): A split-explicit, free- surface, topography-following-coordinate oceanic model. Ocean Modelling 9 (2005) 347-404. https://doi.org/10.1016/j.ocemod.2004.08.002

[9] Miyazawa, Y., Zhang, R., Guo, X., Tamura, H., Ambe, D., Lee, J., Okuno, A., Yoshinari, H., Setou, T., Komatsu, K.: Water mass variability in the western North Pacific detected in a 15-year eddy resolving ocean reanalysis. Journal of Oceanography 65 (2009) 737-756. https://doi.org/10.1007/s10872-009-0063-3

[10] Kamidaira, Y., Uchiyama, Y., Mitarai, S. Eddy-induced transport of the Kuroshio warm water around the Ryukyu Islands in the East China Sea. Continental Shelf Research 143 (2017) 206-218. https://doi.org/10.1016/j.csr.2016.07.004

[11] Blaas, M., Dong, C., Marchesiello, P., McWilliams, J.C., Stolzenbach, K.D.: Sediment-transport modeling on Southern Californian shelves: A ROMS case study. Continental Shelf Research 27 (2007) 832-853. https://doi.org/10.1016/j.csr.2006.12.003

[12] Kim, J.I., Nakatsuji, K., Ishizuka, M.: Relationship between residual current system and the formation mechanism of Okinose sandbank in Osaka Bay. Proceedings of the Coastal Engineering, JSCE 44 (1997) 406-410 (in Japanese).